J|A|C|S
ARTICLES
Published on Web 03/31/2007

# Mapping the Orientation of Helices in Micelle-Bound Peptides by Paramagnetic Relaxation Waves

Michal Respondek, Tobias Madl, Christoph Göbl, Regina Golser, and Klaus Zangger*

*Contribution from the Institute of Chemistry/Organic and Bioorganic Chemistry, University of Graz, Heinrichstrasse 28, A-8010 Graz, Austria*

Received December 15, 2006; E-mail: klaus.zangger@uni-graz.at

***Abstract:*** Many antimicrobial peptides form α-helices when bound to a membrane. In addition, around 80% of residues in membrane-bound proteins are found in α-helical regions. The orientation and location of such helical peptides and proteins in the membrane are key factors determining their function and activity. Here we present a new solution state NMR method for obtaining the orientation of helical peptides in a membrane-mimetic environment (micelle-bound) without any chemical perturbation of the peptide−micelle system. By monitoring proton longitudinal relaxation rates upon addition of the freely water-soluble and inert paramagnetic probe Gd(DTPA-BMA) to an α-helical peptide, a wavelike pattern with a periodicity of 3.6 residues per turn is observed. The tilt and azimuth (rotation) angle of the helix determine the shape of this paramagnetic relaxation wave and can be obtained by least-square fitting of measured relaxation enhancements. Results are presented for the 15-residue antimicrobial peptide CM15 which forms an amphipathic helix almost parallel to the surface of the micelle. Thus, a few fast experiments enable the identification of helical regions and determination of the helix orientation within the micelle without the need for covalent modification, isotopic labeling, or sophisticated equipment. This approach opens a path toward the topology determination of α-helical membrane−proteins without the need for a complete NOE-based structure determination.

## Introduction

Membrane-bound peptides and proteins constitute a major class of all expressed peptides and proteins which are encoded in a genome and are involved in crucial biological processes.[1] In contrast to soluble counterparts far fewer 3D structures of membrane-bound peptides and proteins have been reported.[2−4] NMR spectroscopy has been successful in the structure determination of only a few peptides and mostly $\beta$-barrel type membrane proteins.[5] Considering that approximately 80% of residues in membrane-bound antimicrobial peptides[6,7] and integral membrane proteins are found in α-helices,[8] structural studies of these α-helical membrane-bound biopolymers are currently vastly underrepresented. In addition to the structure the mode of interaction with the membrane is essential in order to elucidate the molecular details of its function. Membrane-mimetic environments typically used for solution NMR studies are micelles or bicelles.[5,9,10] Determining the orientation of helical peptides in a micelle would help in better understanding the still somewhat elusive mechanisms of antimicrobial peptides.[6] For membrane-bound proteins it would provide a topological map of α-helices, which already goes a long way toward its complete 3D structure.

A few methods for the determination of the angular orientation of membrane-bound peptides have been described so far. Most of them employ nuclear or electron spins to determine the orientation of the peptide. Some approaches make use of the observation that oxygen partitions with increasing concentration toward the center of membranes under high pressure.[11] The immersion depth can be investigated by the paramagnetic relaxation induced by oxygen on covalently attached spin labels, fluorine probes, and even protons by ESR as well as $^{19}$F and $^{1}$H NMR.[11−16] The labels are directly linked to cysteine residues, which are incorporated, via mutagenesis, into the position of

(1) Krogh, A.; Larsson, B.; von Heijne, G.; Sonnhammer, E. L. *J. Mol. Biol.* **2001**, *305*, 567−80.
(2) Jiang, J.; Daniels, B. V.; Fu, D. *J. Biol. Chem.* **2006**, *281*, 454−460.
(3) Okumura, H.; Murakami, M.; Kouyama, T. *J. Mol. Biol.* **2005**, *351*, 481−495.
(4) Pornillos, O.; Chen, Y.-J.; Chen, A. P.; Chang, G. *Science* **2005**, *310*, 1950−1953.
(5) Arora, A.; Tamm, L. K. *Curr. Opin. Struct. Biol.* **2001**, *11*, 540−7.
(6) Brogden, K. A. *Nat. Rev. Microbiol.* **2005**, *3*, 238−50.
(7) Strandberg, E.; Ulrich, A. S. *Concept. Magn. Reson. A* **2004**, *23*(A), 89−120.
(8) Mesleh, M. F.; Lee, S.; Veglia, G.; Thiriot, D. S.; Marassi, F. M.; Opella, S. J. *J. Am. Chem. Soc.* **2003**, *125*, 8928−35.
(9) Damberg, P.; Jarvet, J.; Graslund, A. *Methods Enzymol.* **2001**, *339*, 271−85.
(10) Kallick, D. A.; Tessmer, M. R.; Watts, C. R.; Li, C. Y. *J. Magn. Reson. B* **1995**, *109*, 60−5.
(11) Prosser, R. S.; Luchette, P. A.; Westerman, P. W. *Proc. Natl. Acad. Sci. U.S.A.* **2000**, *97*, 9967−71.
(12) Bhargava, K.; Feix, J. B. *Biophys. J.* **2004**, *86*, 329−336.
(13) Evanics, F.; Hwang, P. M.; Cheng, Y.; Kay, L. E.; Prosser, R. S. *J. Am. Chem. Soc.* **2006**, *128*, 8256−64.
(14) Luchette, P. A.; Prosser, R. S.; Sanders, C. R. *J. Am. Chem. Soc.* **2002**, *124*, 1778−1781.
(15) Nielsen, R. D.; Che, K.; Gelb, M. H.; Robinson, B. H. *J. Am. Chem. Soc.* **2005**, *127*, 6430−42.
(16) Prosser, R. S.; Luchette, P. A. *J. Magn. Reson.* **2004**, *171*, 225−32.


**10.1021/ja069004f CCC: $37.00** 

interest. However, the introduction of large reporter groups into peptides might in some cases affect their structural and functional properties. Perhaps the most successful NMR based approach uses dipolar couplings of aligned bilayer samples,[17] weakly aligned micelles,[18] or small bicelles to investigate the positioning of helices in the membrane.[8,19,20] Plotting residual dipolar couplings (RDCs) versus residue number yields dipolar waves which in turn are fitted to a sinusoid corresponding to the helix periodicity.[8,19−21] A detailed analysis of dipolar waves enables determination of absolute (completely aligned samples) or relative (weakly aligned samples)[22] rotation and orientation of helices in the membrane. The need for isotopic labeling and its inherent high cost, especially for peptides commonly prepared by solid-phase synthesis, might prohibit the use of RDCs in some cases. The orientation of a peptide can also be obtained by solid-state NMR by monitoring anisotropic spin interaction tensors as a function of residue number.[23] Depending on the resulting pattern, "chemical shift waves",[24] "quadrupolar waves"[25] or "dipolar waves"[8] have been described based on data obtained from a series of specifically labelled peptide samples.

Limited information about the orientation has also been obtained through relaxation enhancements using paramagnetic groups. These agents can either be covalently linked to the detergent (e.g., phosphocholine) or stay freely soluble in the buffer surrounding the membrane-mimetic environment. In the former case doxyl derivatives of stearic acid are of common use. The spin labels (doxyl groups) have been usually incorporated close to the polar group (position C-5) or the core of the micelle (position C-16) bringing about an enhancement of those residues which are in the proximity of these groups.[26] In the case of water-soluble paramagnetic species the relaxation enhancement affects spins close to the surface of the micelle. As soluble paramagnetic agents, chelate complexes of gadolinium are of common use[26−28] and also nitroxide derivatives like TEMPO[29,30] or salts of $Mn^{2+}$.[31,32] A limitation of this approach is that these commonly used compounds all show interactions with some amino acids or even the micelles.[30] Especially the positively charged manganese ions possess high binding affinity to negatively charged areas on the membrane or protein. These interactions together with typically only rough estimations of relaxation enhancements through peak width measurements resulted in paramagnetic relaxation enhancements (PREs) which provided little information about the actual positioning. The PRE values were more influenced by specific interactions with the soluble paramagnetic agent and/or the spatial indeterminacy of the paramagnetic spin label. In favorable cases it was only possible to distinguish between surface bound and transmembrane orientations of a peptide. Yet, never a detailed picture of the orientation of the peptide in the membrane was obtained.

Here we present a novel method for identifying and orientationally characterizing helical regions of a peptide within a micelle based on accurate relaxation enhancements obtained with the inert and water-soluble paramagnetic relaxation agent gadolinium-diethylenetriamine pentaacetic acid-bismethylamide Gd(DTPA-BMA).[33] These accurate experimental PREs correlate very well with the calculated insertion depths of residues in helical peptides thus allowing the extraction of tilt and azimuth angles. Using this approach we determined the orientation of the α-helical 15-residue peptide CM15[34] in dodecyl-phosphocholine (DPC) micelles. The presented method should also prove useful in the orientation mapping of other kinds of structurally defined compounds embedded in a large molecular assembly as long as the molecule to be studied can be NMR spectroscopically assigned.

## Experimental Section

**Materials.** CM15 (sequence:KWKLFKKIGAVLKVL) was made by FMOC-based solid-phase peptide synthesis and purchased from Peptide Specialty Laboratories GmbH (Heidelberg, Germany). DPC-$d_{38}$ (98%) was from Cambridge Isotope Laboratories Inc. (Andover, MA). Gd(DTPA-BMA) was purified from the commercially available MRI contrast reagent Omniscan (Nycomed, Oslo, Norway) by fast-performance liquid chromatography (FPLC). Omniscan was diluted with water to 250 mM and chromatographed by an Äkta Purifier (Amersham Biosciences, Uppsala, Sweden). The isocratic separation was performed on a semipreparative $C_{18}$ reversed phase (RP) column (Lichrospher 100 RP-18, 250 mm × 10 mm, particle size 10 μm, Merck, Germany). The mobile phase was 80% water and 20% acetonitrile at a flow rate of 2 mL/min. Detection was performed with a variable wavelength detector set at 190 nm. Injection volume was 100 μL. Gd(DTPA-BMA) was eluted as a single peak ($t_R$ 6.2 min). The fractions were combined and lyophilized to afford a white amorphous powder. Purified Gd(DTPA-BMA) can be obtained from the authors upon request. All other chemicals were from Sigma-Aldrich (St.Louis, MO) in the highest purity available.

**NMR Spectroscopy.** All experiments were carried out on a Bruker Avance DRX 500 MHz spectrometer equipped with an HX inverse probe with *z*-axis gradients at 305 K. Samples of 1.7 mM CM15 dissolved in 100 mM DPC-$d_{38}$, 50 mM phosphate buffer (pH = 5.0) including 10% $D_2O$ and 0.02% sodium azide were used. For the assignment and solution structure determination we used TOCSY and NOESY spectra with mixing times of 40 and 150 ms, respectively. The solvent signal was suppressed using two excitation sculpting blocks before the start of the acquisition. Partial assignment of $^{13}C$ chemical shifts was accomplished with an $^{1}H-^{13}C$ HSQC for which 352 scans were acquired for each of the 256 increments.

To obtain paramagnetic relaxation enhancements the CM15 sample was titrated with Gd(DTPA-BMA) (60 mM) to final concentrations of 1, 2, 3, 4, 5, 7.5, 10, and 12.5 mM. Proton $T_1$ relaxation times were

(17) Marassi, F. M.; Ramamoorthy, A.; Opella, S. J. *Proc. Natl. Acad. Sci. U.S.A.* **1997**, *94*, 8551−6.
(18) Chou, J. J.; Kaufman, J. D.; Stahl, S. J.; Wingfield, P. T.; Bax, A. *J. Am. Chem. Soc.* **2002**, *124*, 2450−2451.
(19) Mesleh, M. F.; Opella, S. J. *J. Magn. Reson.* **2003**, *163*, 288−299.
(20) Mesleh, M. F.; Veglia, G.; De Silva, T. M.; Marassi, F. M.; Opella, S. J. *J. Am. Chem. Soc.* **2002**, *124*, 4206−4207.
(21) Mascioni, A.; Eggimann, B. L.; Veglia, G. *Chem. Phys. Lipids* **2004**, *132*, 133−44.
(22) Veglia, G.; Opella, S. J. *J. Am. Chem. Soc.* **2000**, *122*, 11733−11734.
(23) Andronesi, O. C.; Becker, S.; Seidel, K.; Heise, H.; Young, H. S.; Baldus, M. *J. Am. Chem. Soc.* **2005**, *127*, 12965−74.
(24) Kovacs, F. A.; Denny, J. K.; Song, Z.; Quine, J. R.; Cross, T. A. *J. Mol. Biol.* **2000**, *295*, 117−25.
(25) van der Wel, P. C.; Strandberg, E.; Killian, J. A.; Koeppe, R. E., II. *Biophys. J.* **2002**, *83*, 1479−88.
(26) Hilty, C.; Wider, G.; Fernandez, C.; Wuethrich, K. *ChemBioChem* **2004**, *5*, 467−473.
(27) Appelt, C.; Wessolowski, A.; Soderhall, J. A.; Dathe, M.; Schmieder, P. *ChemBioChem* **2005**, *6*, 1654−62.
(28) Bernini, A.; Spiga, O.; Venditti, V.; Prischi, F.; Bracci, L.; Tong, A. P.; Wong, W. T.; Niccolai, N. *J. Am. Chem. Soc.* **2006**, *128*, 9290−1.
(29) Esposito, G.; Lesk, A. M.; Molinari, H.; Motta, A.; Niccolai, N.; Pastore, A. *J. Mol. Biol.* **1992**, *224*, 659−70.
(30) Petros, A. M.; Mueller, L.; Kopple, K. D. *Biochemistry* **1990**, *29*, 10041−8.
(31) Porcelli, F.; Buck, B.; Lee, D. K.; Hallock, K. J.; Ramamoorthy, A.; Veglia, G. *J. Biol. Chem.* **2004**, *279*, 45815−23.
(32) Schievano, E.; Calisti, T.; Menegazzo, I.; Battistutta, R.; Peggion, E.; Mammi, S.; Palu, G.; Loregian, A. *Biochemistry* **2004**, *43*, 9343−51.
(33) Pintacuda, G.; Otting, G. *J. Am. Chem. Soc.* **2002**, *124*, 372−3.
(34) Andreu, D.; Ubach, J.; Boman, A.; Wahlin, B.; Wade, D.; Merrifield, R. B.; Boman, H. G. *FEBS Lett.* **1992**, *296*, 190−4.

obtained from a series of 2D NOESY spectra with a saturation recovery sequence at the beginning. Typically eight such 2D data sets were acquired with recovery delays of 100, 300, 500, 700, 1000, 1500, 2000, and 3000 ms. Subsequently, the peak intensities were fitted to

$$I = I_0(1 - e^{-t/T_1}) \quad (1)$$

to obtain the relaxation times $T_1$. All spectra were processed using nmrPipe[35] and analyzed by NMRViewJ.[36]

**Structure Calculation.** NOESY cross-peaks of CM15 were assigned manually, and the peak volumes were integrated with the program NMRViewJ[36] and translated into distance restraints using the built-in median method. Additionally, $\phi$ and $\psi$ dihedral angle restraints were obtained using the program TALOS[37] based on Hα proton as well as Cα and C$\beta$ carbon chemical shifts. A total of 280 NOEs and 23 dihedral angle restraints were used for the structure determination. The structure calculation was carried out with the program CNS[38] using the full simulated annealing method.

## Theoretical Basis

**Paramagnetic Relaxation Waves.** Two parameters are needed to define the orientation of an α-helix in a membrane or membrane-mimetic environment. These are (1) the *tilt angle* $\tau$, which defines the angle between the helix axis and the membrane surface and (2) the *azimuth angle* $\rho$ (also called rotation angle), which defines the rotation of the helix and hence which side chains point toward the interior (see Figure 1). As will be shown, both can be obtained by measuring the relaxation enhancements exerted by a freely soluble and inert paramagnetic probe on nuclei along the backbone of the helix. In micellar systems we define the tilt angle $\tau$ between the helix axis and a normal to the line connecting the center of the helix with the center of the micelle.

For our analysis we start by describing the immersion depth $d$ of a particular nucleus on the backbone of an α-helix by

$$d = A + 1.5\ \text{Å} \sin\tau(x - 1) - \cos(\tau)\, B \cos(1.745(x - 1) + \rho) \quad (2)$$

where the dependent variable $x$ is the residue number. $A$ is the immersion depth of the helical axis at the position of the first residue. The second term 1.5 Å sin($\tau$) ($x$ − 1) describes the increasing membrane insertion by going along the peptide chain when the tilt angle is larger than zero. The factor of 1.5 is the helical pitch (in Å) per residue. The third term in eq 2 accounts for the oscillating helical behavior and is given by cos(1.745$x$ + $\rho$), where 1.745$x$ is equal to $(2\pi)/(3.6)x$ and defines the periodicity of 3.6 residues per turn. $B$ is the radius of the helix measured at the site of the nuclei under study. For a typical α-helical geometry this radius is 3.25 Å when measured at the site of Hα protons and 1.95 Å for NHs. The enhancement of longitudinal relaxation rates exerted by a single paramagnetic center on a nucleus at a distance of $r$, also known as paramagnetic relaxation enhancement (PRE), is given by[39]

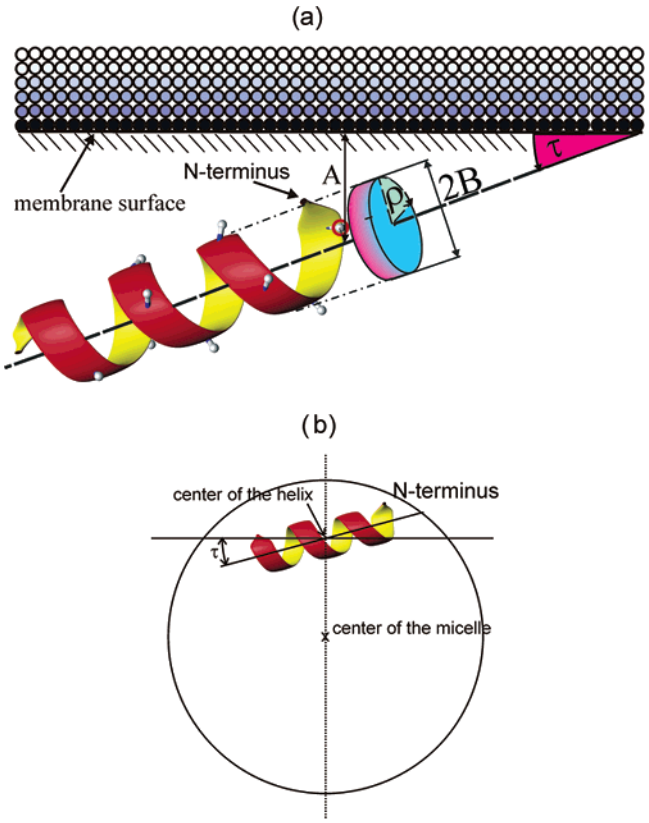


***Figure 1.*** Parameters used for the description of paramagnetic relaxation rates on helical peptides in membranes (a) and for the definition of the tilt angle in micellar systems (b). The tilt angle $\tau$ is defined between the membrane surface and the helical axis. The azimuth angle $\rho$ is measured between the first α-proton and a line, which is perpendicular to the helix axis and points toward the membrane surface. The diminishing influence of freely soluble paramagnetic agents on the relaxation rates is drawn by decreasing color depths outside the membrane.

$$PRE = \frac{a}{r^6} \quad (3)$$

with "$a$" being a combination of various constants. Nuclei closer to the paramagnetic agent experience higher relaxation enhancements and the influence drops off rapidly with increasing distance. If there is no specific interaction between the molecule under study and the paramagnetic center, the influence of the electron on nuclear relaxation can be described by the "outer sphere" relaxation approach.[39] In this case the nucleus−electron distances can be considered frozen on the time scale of electron relaxation and the PRE values are obtained by simple integration over the whole volume occupied by paramagnetic probes. For a planar membrane surrounded by a buffer containing a noninteracting paramagnetic probe, the total paramagnetic relaxation enhancement of a nucleus with immersion depth $d$ is given by the integral over all paramagnetic molecules weighted by $1/r^6$ and multiplied by the probability of finding a paramagnetic center in a particular volume element. This occupancy of paramagnetic elements which is proportional to the macroscopic concentration of a paramagnetic molecule is combined with the constant "$a$" into a new constant "$k$" to yield a relaxation enhancement of

$$\text{PRE} = \int_{d+l}^{\infty}\int_{-\infty}^{\infty}\int_{-\infty}^{\infty} \frac{k}{r(x,y,z)^6}\, dx\, dy\, dz \quad (4)$$

(35) Delaglio, F.; Grzesiek, S.; Vuister, G. W.; Zhu, G.; Pfeifer, J.; Bax, A. *J. Biomol. NMR* **1995**, *6*, 277−93.
(36) Johnson, B. A.; Blevins, R. A. *J. Biomol. NMR* **1994**, *4*, 603−614.
(37) Cornilescu, G.; Delaglio, F.; Bax, A. *J. Biomol. NMR* **1999**, *13*, 289−302.
(38) Brunger, A. T.; Adams, P. D.; Clore, G. M.; DeLano, W. L.; Gros, P.; Grosse-Kunstleve, R. W.; Jiang, J. S.; Kuszewski, J.; Nilges, M.; Pannu, N. S.; Read, R. J.; Rice, L. M.; Simonson, T.; Warren, G. L. *Acta Crystallogr., Sect. D* **1998**, *54*, 905−21.
(39) Bertini, I.; Luchinat, C.; Parigi, G. *Solution NMR of Paramagnetic Molecules*; Elsevier: 2001.

where $r(x,y,z)$ is the distance between the nucleus and the paramagnetic center. The integration in the $x$-direction (perpendicular to the membrane surface) starts at $d + l$, where $l$ includes the solvent layer and the radius of the paramagnetic probe. Integration of eq 4 yields

$$\mathrm{PRE} = \frac{k\pi}{6(d+l)^3} \tag{5}$$

when expressed as a function of the immersion depth $d$. Equation 5 can be used only when the influence from one surface has to be considered. In the more general case of a bilayer, the paramagnetic relaxation enhancements from both surfaces have to be added, leading to

$$\mathrm{PRE} = \frac{k\pi}{6(d+l)^3} + \frac{k\pi}{6(D-(d+l))^3} \tag{6}$$

where $D$ is the diameter of the membrane. Equations 5 and 6 hold for a planar membrane. However, a very similar dependence can be obtained by a numerical grid search for spherical micelles in the size range typically used by solution NMR, as shown in the Supporting Information.

We now define $y = d + l$ as the affective immersion depth and use it to describe the helical wave eq 2. Thus, only parameter $A$ changes to the affective immersion depth $(d + l)$ of the first residue. Substituting eq 2 into eq 5 yields the paramagnetic relaxation enhancement described in terms of helix positioning parameters

$$\mathrm{PRE} = \frac{k\pi}{6\left(\begin{array}{c} A + 1.5\ \text{Å} \cdot \sin\tau \cdot (x-1) - \\ \cos(\tau) \cdot B \cdot \cos(1.745 \cdot (x-1) + \rho) \end{array}\right)^3} \tag{7}$$

or for bilayers (substituting eq 2 in eq 6)

$$\mathrm{PRE} = \frac{k\pi}{6\left(\begin{array}{c} A + 1.5\ \text{Å} \cdot \sin\tau \cdot (x-1) - \\ \cos(\tau) \cdot B \cdot \cos(1.745 \cdot (x-1) + \rho) \end{array}\right)^3} + \frac{k\pi}{6\left(D - \left(\begin{array}{c} A + 1.5\ \text{Å} \cdot \sin\tau \cdot (x-1) - \\ \cos(\tau) \cdot B \cdot \cos(1.745 \cdot (x-1) + \rho) \end{array}\right)\right)^3} \tag{8}$$

Equations 7 and 8 can be used to fit the measured relaxation enhancements as a function of residue number to obtain the exact positioning of a helical peptide in a membrane. These equations are exact solutions for planar membranes. However, due to the similar PRE vs $r$ behavior of micelles, eqs 7 and 8 can also be used for small helices bound to these membrane-mimetic systems.

## Results and Discussion

The 15-residue peptide CM15 used for this study is a hybrid peptide of cecropin A (residues 1−7) and mellitin (residues 2−9). It was recognized as a peptide with a minimal sequence which displays antimicrobial activity,[34] most likely due to formation of an amphipathic α-helical structure upon binding to membranes.[40] Upon dissolution in an aqueous buffer it showed a poor chemical shift dispersion typical for random coil peptides.[41] Addition of DPC-$d_{38}$ led to large shift changes up to concentrations of around 70 mM DPC. To ensure that all the peptide is bound to micelles a concentration of 100 mM DPC was used subsequently, corresponding to ∼60 equiv of DPC per peptide molecule. Proton signals were assigned using TOCSY, NOESY, and $^1$H−$^{13}$C HSQC spectra. The solution structure was determined using 280 NOEs, together with 23 dihedral angle restraints which were obtained using the program TALOS with chemical shifts of Hα, Cα, and C$\beta$ nuclei. During a later stage in the structure refinement C′O to NH hydrogen bond restraints were introduced for α-helical residues based on their typical NOE pattern, chemical shifts, and TALOS-derived $\phi$ and $\psi$ angles. The structure of CM15 bound to DPC micelles has been deposited in the PDB data base under accession number 2JMY. A total of 40 structures were calculated, and the 20 lowest energy structures are shown in Figure 2 as a least-square fit bundle. Residues 4−14 form a well-defined α-helical structure with a remarkably low backbone rmsd of 0.14 Å. While a few low-intensity NOEs typical for an α-helix were also found for residues 2−4, their chemical shifts were not typical for an α-helix. In addition, these residues also had narrower signals indicating enhanced flexibility. In the resulting structure the first few residues are still arranged in a helical fashion, but their geometry is not characteristic of an α-helix (Figure 2).

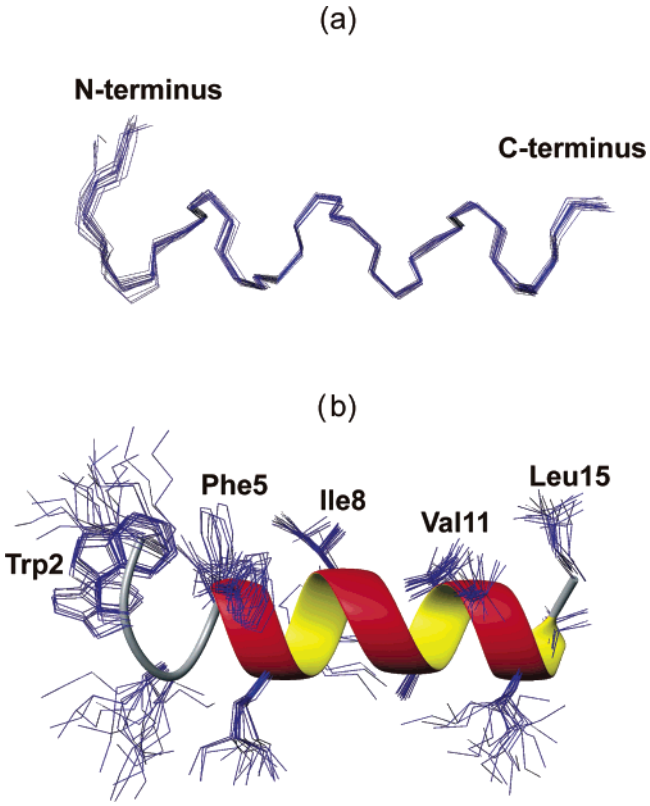


***Figure 2.*** Superposition of the backbones of 20 lowest-energy structures of CM-15 in DPC micelles (a). A ribbon diagram of the closest-to-mean structure together with side-chain bundles is shown in (b). Hydrophobic residues are labeled.

In order to determine the relative orientation (tilt angle) and rotation (azimuth angle) of CM15 in DPC micelles, a titration of the peptide−DPC micelle complex with Gd(DTPA-BMA) was performed. Among many available paramagnetic species,

(40) Zasloff, M. *Nature* **2002**, *415*, 389−395.

(41) Wüthrich, K. *NMR of Proteins and Nucleic Acids*; Wiley: New York, 1986.

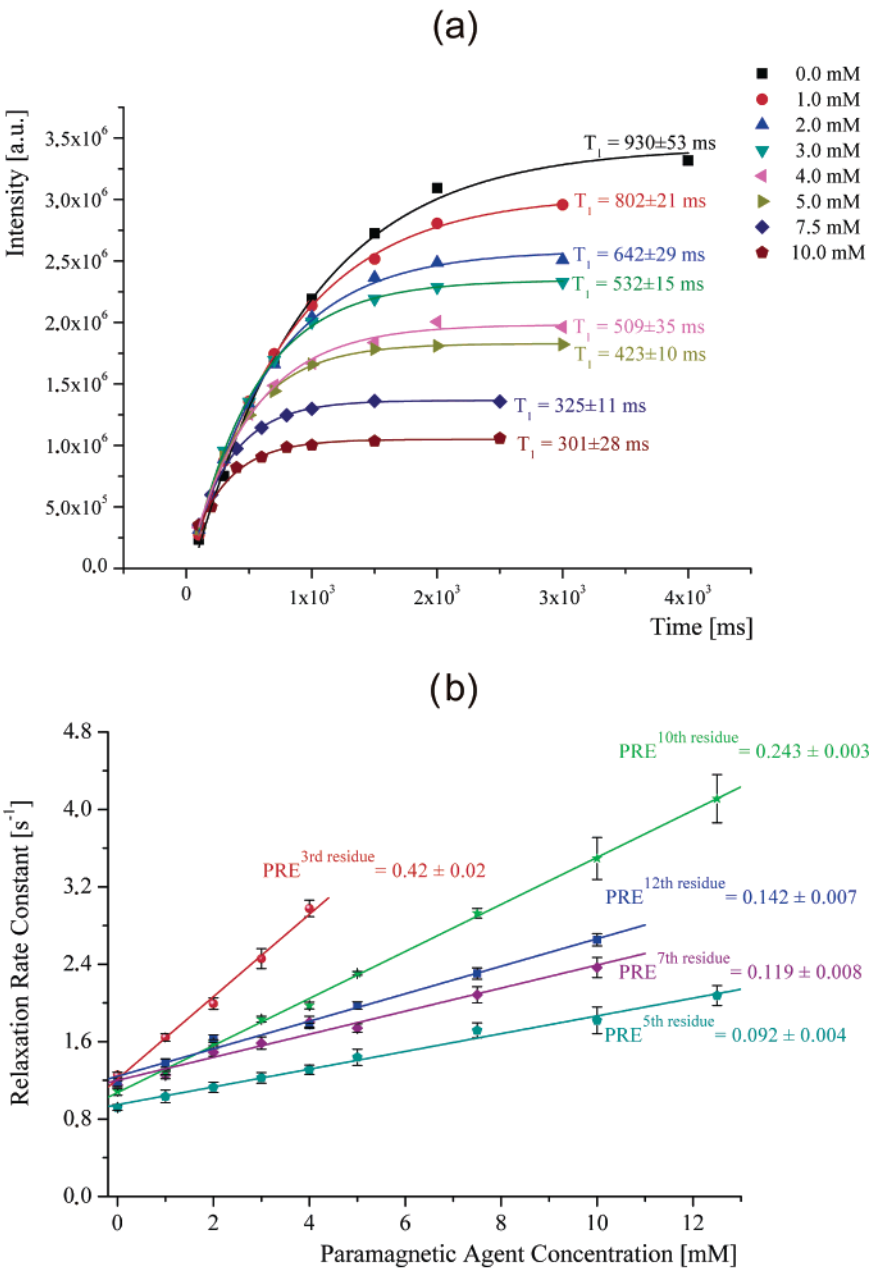


***Figure 3.*** Influence of the concentration of Gd(DTPA-BMA) on the signal presaturation recovery of Ala10-Hα is shown in (a), while paramagnetic relaxation enhancements of representative Hα protons is shown in (b). The intensity in (a) is given in arbitrary units.

Gd(DTPA-BMA) seemed to be the most suitable for our experiments due to its high solubility in water and its absence of interactions with proteins.[33] Upon addition of Gd(DTPA-BMA) to final concentrations up to 12.5 mM, no shifts of resonances were detected, confirming the absence of specific interactions with the peptide or micelle.

At each step of the titration a set of eight *saturation-recovery* 2D-NOESY spectra were recorded. The delay between presaturation and start of the NOESY sequence was between 100 and 3000 ms. Proton $T_1$ relaxation times were obtained by fitting the measured intensities to eq 1. Correlation coefficients were usually around 0.99, and representative examples are shown in Figure 3a. Plotting relaxation times as a function of Gd(DTPA-BMA) concentration yields a straight line whose slope is the paramagnetic relaxation enhancement. As can be seen in Figure 3b, clearly distinguishable values of the relaxation enhancements were found for different protons. It should be noted that in general one does not need to carry out a full titration with Gd-(DTPA-BMA). Instead, acquiring relaxation times in the absence and presence of a significant concentration of the paramagnetic agent should suffice. However, the titration was carried out to prove its linear behavior.

Drawing the observed PRE values of Hα protons as a function of the residue number (see Figure 4) results in a wavelike pattern between residues 5 and 15, whereas the first 3 residues are characterized by highly enhanced values. The wavelike pattern, which we call a "paramagnetic relaxation wave", can be fit to eq 7 or 8 to obtain the orientational parameters $\tau$ and $\rho$. The tilt angle of $-14 \pm 6°$ corresponds to a helix orientation almost parallel to the surface. The negative sign means that the C-terminus is closer to the surface than the N-terminus. The azimuth angle $\rho$ determines the rotation of the helix. This angle

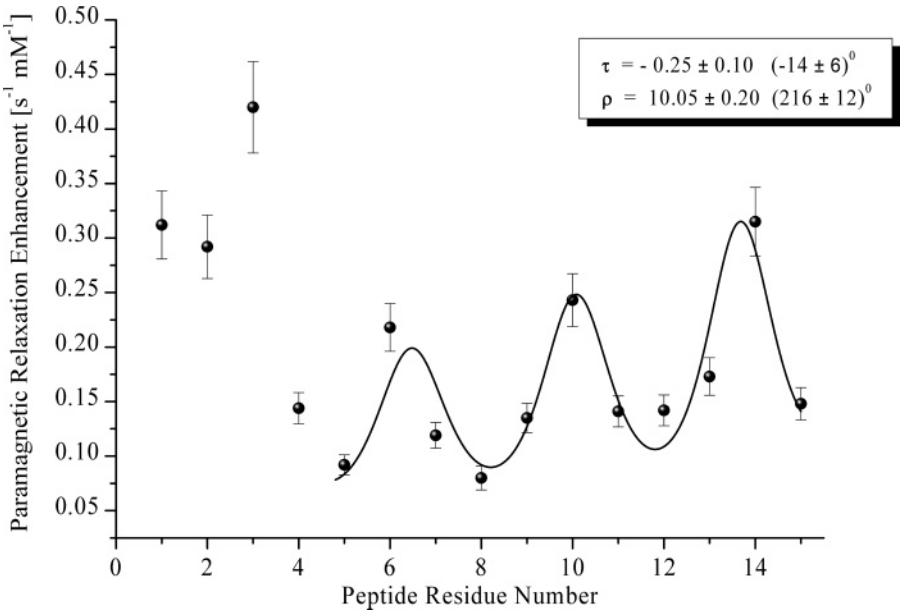


***Figure 4.*** PRE values of Hα nuclei of CM-15 as a function of residue number. The sinusoidal behavior between residues 5 and 15 was least-square fitted to eq 7 to yield the tilt and azimuth angles as indicated.

is measured from the point closest to the surface (12 o'clock position). So, 0° and 180° correspond to orientations of the first residue toward the surface and interior of the membrane, respectively. A $\rho$-value of 216 ± 12° means that the first residue used in the paramagnetic relaxation wave fit (residue number 5 of CM15) is pointing approximately to the center of the micelle. The paramagnetic relaxation wave (Figure 4) shows that residues Phe5, Ile8, Leu12, and Leu15 are located deep in the micelle, which is in good agreement with their hydrophobicity.

The small tilt angle obtained from the paramagnetic relaxation wave (Figure 4) is in accordance with the parallel orientation of the peptide relative to the surface as found by a previous solid-state NMR investigation observing oxygen accessibility on six individually introduced spin labels in CM15.[12] In this study no specific values for tilt or azimuth angles have been reported. However, the wavelike pattern obtained in this study through a series of mutant CM15 peptides is in very good agreement with our paramagnetic relaxation wave using an unmodified peptide. Some PREs (for residues 6, 7, and 12) show larger deviations from the fitted values (see Figure 4). These differences can be explained by signal overlap (the Hα protons of residues 7 and 12 are partially overlapped by other signals) or low signal-to-noise ratios (NOEs observed for the Hα of residue 6 have the lowest intensities of all Hα protons). Helical regions in peptides can be identified by paramagnetic relaxation waves without a complete structure determination and only require sequence-specific backbone assignments. Therefore, they represent a fast way of identifying the sequence localization and topology of α-helices, especially if the tilt angle is not too large. A paramagnetic relaxation wave as found for CM15 (Figure 4) is typical for an orientation parallel to the surface. The sinusoidal part of this function becomes less pronounced when the tilt angle increases. Calculated PRE values as a function of residue number for various positive tilt angles (from parallel to the surface to transmembrane) are shown in Figure 5.

These curves were calculated using eq 8 for a planar membrane and are similar for small helices in micellar systems.

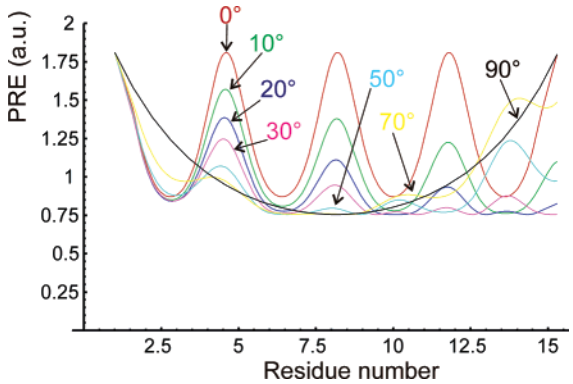


***Figure 5.*** Paramagnetic relaxation waves calculated using eq 8 as a function of tilt angle. Tilt angles are indicated from parallel to the surface (red, $\tau$ = 0°) to transmembrane (black, $\tau$ = 90°).

Small changes in tilt and azimuth angle lead to significantly modified paramagnetic relaxation waves. Therefore, in some cases it will probably suffice to compare the measured PRE values with these calculated paramagnetic relaxation waves in order to get a rough estimation of helix orientation. For tilt angles close to 90° the wavelike patterns disappears. However, in the case of transmembrane helices the change of PREs as a function of residue number is much slower than that for, e.g., an extended $\beta$-strand type conformation and should thus still provide enough information about the presence of an helical region.

Besides the backbone, PRE values could also be obtained for some of the side-chain protons. In Figure 6 the peptide is drawn as a ball-and-stick model, color-coded by the PRE values, with red indicating high values and therefore close proximity to the surface of the micelle.

The peptide is bound close and basically parallel to the surface of the micelle. As already found for backbone protons, the side chain signals of the first three residues also show highly elevated values indicating an orientation pointing away from the center of the micelle. This seems surprising considering the almost α-helical arrangement in the NOE based structure. However,

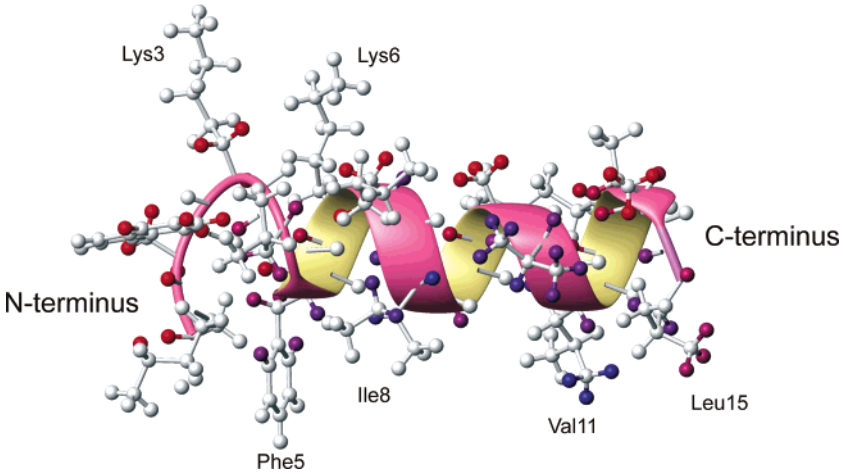


***Figure 6.*** Ball-and-stick model of CM15, color-coded with PREs ranging from blue (low values) to red (high PREs). Protons for which PREs could not be obtained unambiguously, because of signal overlap, are left white. Some exposed residues are annotated.

as mentioned above these residues showed also rather narrow signals and only a few and weak NOEs. If a flexible peptide adopts a conformation where it is oriented toward the surface for a short period of time or even sticks out of the micelle, the PREs will be averaged in favor of high values. This is due to the $1/d^3$ weighting of PRE values, where $d$ is the distance from the paramagnetic layer. On the other hand NOEs are averaged with a $1/r^6$ dependence ($r$ being the proton−proton separation) toward short H−H distances. Consequently, a partial α-helical conformation will lead to NOEs typical for this secondary structural element, while a conformation pointing toward the solution will not lead to any significant NOEs. In other words, conformational heterogeneity (or flexibility) is interpreted in different ways by NOEs and PREs. While NOEs emphasize a closed conformation, PREs show mainly an open form. It can be argued that the error introduced is larger by NOEs as they are $1/r^6$ weighted, while PREs by a soluble paramagnetic agent are weighted only by $1/d^3$. Discrepancies between NOEs and PREs are indicative of a flexible region, and thus PRE values could also be used to obtain information about the dynamical behavior of micelle-bound peptides.

## Conclusions

We have shown that helical regions in peptides can be identified and the orientation of the helix be obtained using relaxation enhancements induced by a paramagnetic agent that is freely soluble and inert toward peptides and the micelle-forming detergent. Since this method does not imply any covalent modification of the peptide or micelle there is no perturbation of the peptide−lipid interaction. In addition isotopic labeling of the peptide is not required, as long as it can be assigned using homonuclear NMR techniques. If $^{15}$N- and $^{13}$C-labeled peptides/proteins are available it constitutes a very fast way to determine the topology of α-helices within the membrane-mimetic environment. While in the presented work relaxation enhancements obtained with the inert paramagnetic probe Gd-(DTPA-BMA) have been used to define the exact orientation of helical peptides in micelles, this approach provides positioning information for any kind of peptide or proteins bound to a membrane-mimetic environment. This opens the door for a wide range of applications in defining micelle/membrane-bound peptide/protein structures. Furthermore, the applicability of the presented method is of course not restricted to peptides and proteins bound to a micelle but should prove useful whenever a ligand (e.g., organic, natural products) is positioned in any large molecular complex of defined shape.

**Acknowledgment.** Financial support by the Austrian Science Foundation (FWF) under Project Nos. 17231 and 14847 to K.Z. is gratefully acknowledged. T.M. thanks the Austrian Academy of Sciences for a DOC scholarship.

**Supporting Information Available:** Mathematical derivation of paramagnetic relaxation enhancements for a micelle system; a graphical comparison of calculated PRE vs immersion depth curves for planar membranes and micelles. This material is available free of charge via the Internet at http://pubs.acs.org.

JA069004F